

Constraining the post-emissions temperature change

Nathaniel Tarshish (✉ tarshish@berkeley.edu)

UC Berkeley

Nadir Jeevanjee

Geophysical Fluid Dynamics Laboratory

Inez Fung

University of California, Berkeley

Article

Keywords:

Posted Date: April 5th, 2022

DOI: <https://doi.org/10.21203/rs.3.rs-1519965/v1>

License: © ⓘ This work is licensed under a Creative Commons Attribution 4.0 International License.

[Read Full License](#)

Constraining the post-emissions temperature change

Nathaniel Tarshish¹, Nadir Jeevanjee², Inez Fung¹

April 3, 2022

Climate models predict that if CO₂ emissions ceased today, the current temperature anomaly of $\sim 1^\circ\text{C}$ would likely persist for thousands of years. Extending a widely-used energy balance model of Earth’s climate to the case of emissions cessation reveals how this post-emissions response is governed by the equilibrium climate sensitivity, transient climate response, and CO₂ airborne fraction. Temperature invariance after emissions cessation is found to be particular to the historical rate of emissions, and is therefore not a fundamental property of climate.

The global mean temperature has increased by roughly 1°C due to greenhouse gases emitted by human activities since the late 1800s¹. Whether or not these historical emissions commit us to future increases in temperature is a fundamental question in climate science. The societal enterprise of pursuing temperature targets (e.g., the Paris Agreement) demands an answer^{2,3}.

It is expected that, following emissions cessation, the atmospheric CO₂ concentration will decline due to land and ocean uptake, yielding a reduction in surface radiative heating. At present, radiative heat primarily flows from the surface ocean into the deep ocean. As the deep ocean gradually warms, however, its role as a heat sink for the surface will diminish. Whether the surface temperature increases, stays the same, or decreases will depend on how the heat source (greenhouse gas radiation) changes relative to the heat sink (mixing with the deep ocean)^{4,5}.

Numerous climate model simulations⁴⁻⁹ have been performed to map out the post-emissions temperature for various emissions scenarios, and have observed each of the three behaviors. The majority of studies, however, find that the post-emissions change in temperature is small relative to the temperature anomaly at emissions cessation. This had led to the view that historical emissions do not commit us to significant future warming. The CMIP6 inter-comparison project⁶ reached this conclusion again after analyzing the post-emissions temperature change over the century following cessation in state-of-the-art models. Here, we examine the temperature response over the *millennium* following emissions and address three basic questions about the long-term post-emissions climate:

1) Why, on average, do models remain at the same temperature after emissions cease? It is unclear if this behavior holds for general emissions scenarios, and is thus a fundamental property of climate, or if it is particular to historical emissions.

2) How is this behavior consistent with our broader understanding of climate? Past efforts⁶ to relate the post-emissions temperature change to established climate metrics, such as the equilibrium climate sensitivity (ECS), transient climate response (TCR), and transient climate response to cumulative emissions (TCRE), found poor correlations. The post-emissions temperature change appears to be largely unconstrained by conventional measures of climate (Extended Data Fig. 1).

3) Which key differences between models are responsible for inter-model spread in the post-emissions temperature? In particular, the relative contributions of climate physics (e.g., cloud feedbacks or ocean mixing) versus the carbon uptake are unknown.

Investigating these questions calls for a simple quantitative model for the phenomenon. Here we advance our understanding by deriving an analytic theory for the long-term committed temperature change in an idealized energy balance model. Despite its simplicity, our results reproduce comprehensive climate model simulations to first order, and inspection of the analytic model yields insight into the above questions.

The post-emissions temperature change

The post-emissions temperature change is conventionally known as the zero emissions commitment (ZEC)¹⁰, defined as the difference between the final long-term temperature anomaly T_f and the temperature anomaly at the time of zero emissions T_{ze} :

$$\text{ZEC} = T_f - T_{ze}. \quad (1)$$

Anomalies are taken with respect to pre-industrial. Long term refers to the carbon and temperature equilibria that emerge after substantial deep-ocean mixing over roughly the next millennium.

To constrain ZEC, we appeal to the two-box model of the climate¹¹⁻¹³. The temperature response to radiative forcing can be partitioned into a fast mode of the ocean’s surface layer coupled to a slow mode governed by the deep ocean (Methods). If the deep ocean anomaly is small compared to the surface anomaly at emissions cessation, T_{ze} is determined by the fast surface mode, and can be obtained by scaling the model’s transient climate response (TCR)—the temperature at the time of CO₂ doubling (year 70) following a 1%/yr increase in CO₂ concentration—by the radiative forcing at cessation. This forcing depends logarithmically on the atmospheric CO₂ anomaly $A_{ze}C_{\text{emit}}$, where A_{ze} is the fraction of cumulative emissions C_{emit} present in the atmosphere at zero emissions. The final equilibrium T_f is likewise constrained by scaling the equilibrium climate sensitivity (ECS) by the final radiative forcing. The logarithm of the final CO₂ anomaly A_fC_{emit} , where A_f is the final airborne fraction, determines this final forcing.

Combining these constraints on T_f and T_{ze} (equations (13) and (17) in Methods) yields a novel analytic formula for the zero-

¹ Department of Earth and Planetary Science, University of California, Berkeley, CA, USA, ² Geophysical Fluid Dynamics Laboratory, Princeton, NJ, USA

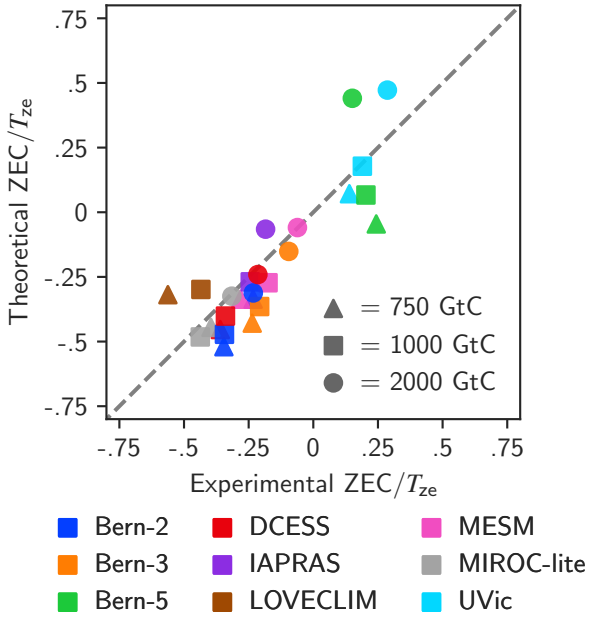


Fig. 1| Comparing ZEC predictions to experiment. Fractional change in the temperature anomaly over the millennium following emissions cessation as realized by EMIC simulations versus the theoretical formula (Eqn. 4) for cumulative emissions of 750 GtC (triangles), 1000 GtC (squares), and 2000 GtC (circles). Prior to zero emissions, models are forced by a 1%/yr increase in CO₂ concentration and emissions are inferred from the carbon budget.

emissions commitment,

$$\text{ZEC} = \frac{1}{\log 2} \left[\log \left(1 + \frac{A_f C_{\text{emit}}}{C_{\text{pre}}} \right) \text{ECS} - \log \left(1 + \frac{A_{ze} C_{\text{emit}}}{C_{\text{pre}}} \right) \text{TCR} \right], \quad (2)$$

where $C_{\text{pre}} \approx 530 \text{ GtC}$ is the pre-industrial mass of atmospheric carbon¹⁴.

Consider the simplifying case of $C_{\text{emit}} < C_{\text{pre}}/A_{ze} \approx 1000 \text{ GtC}$. Linearizing the logarithms yields

$$\text{ZEC} = \frac{1}{\log 2} \left(\frac{C_{\text{emit}}}{C_{\text{pre}}} \right) (A_f \text{ECS} - A_{ze} \text{TCR}). \quad (3)$$

The sign of ZEC can be deduced by comparing A_f/A_{ze} to TCR/ECS . Here A_f/A_{ze} serves as a measure of the disequilibrium in the carbon system when emissions are zeroed. The realized warming TCR/ECS is a proxy for the disequilibrium in the model's thermal response. This idealized model provides a quantitative foundation for the observation in climate models⁹ that the relative degrees of disequilibrium in the carbon and thermal responses impact ZEC.

When $A_f/A_{ze} > \text{TCR}/\text{ECS}$, the carbon system is closer to equilibrium than the thermal response. As a result, the magnitude of the cooling effect from reducing radiative heating due to carbon uptake is less than the surface heating generated by turning off the deep ocean heat sink. In this case, net heating occurs and ZEC is positive. On the other hand, ZEC is negative when $A_f/A_{ze} < \text{TCR}/\text{ECS}$, indicating that the thermal response is closer to equilibrium than the carbon system. A reduction in radiative heating due to carbon uptake dominates the temperature evolution and yields net cooling.

In evaluating the magnitude of ZEC, the temperature anomaly at cessation T_{ze} provides the relevant scale for comparison (Methods),

$$\frac{\text{ZEC}}{T_{ze}} = \frac{\log \left(1 + A_f C_{\text{emit}}/C_{\text{pre}} \right)}{\log \left(1 + A_{ze} C_{\text{emit}}/C_{\text{pre}} \right)} \left(\frac{\text{ECS}}{\text{TCR}} \right) - 1. \quad (4)$$

Taking the small C_{emit} limit again, we find

$$\frac{\text{ZEC}}{T_{ze}} = \frac{A_f/A_{ze}}{\text{TCR}/\text{ECS}} - 1. \quad (5)$$

We conclude that the relative magnitude—in addition to the sign—of the post-emissions deviation is determined by the ratio of the carbon disequilibrium to the thermal disequilibrium. The dependence of ZEC on the emissions scenario enters only through the carbon disequilibrium: A_{ze} is expected to depend on the rate of emissions¹⁵, and A_f is sensitive to the magnitude of cumulative emissions^{16,17}. Carbon uptake also depends on temperature, and while the strength of carbon-climate feedbacks varies across models, their presence increases A_f ^{18,19}. The thermal disequilibrium, however, is a constant, which depends on the climate model but not the emissions scenario. In the two-box model, the thermal disequilibrium is determined by the surface ocean's propensity to cool to space versus cool to deeper waters, and this degree of freedom is fully constrained by diagnosing TCR in the 1%/yr run and comparing to ECS (Methods).

Note that the ZEC formula does not constrain the time-dependent evolution towards equilibrium, and has no bearing on whether transient peak temperatures occur after zero emissions but before the long-term equilibrium. The experiments in the Zero Emissions Commitment Model Intercomparison Project (ZECMIP), however, do not show substantial transient behavior⁶. Of the nine models analyzed here, temperatures monotonically approach the long-term equilibrium in all but one model (IAPRAS) as shown in Extended Data Fig. 2.

Theory reproduces simulations

To understand the accuracy of the idealized treatment, we analyze the ZECMIP experiments⁶ in which the atmospheric CO₂ concentration increases at a rate of 1%/yr until the diagnosed cumulative emissions reach 750, 1000, and 2000 GtC. Temperature and carbon evolutions for the models are plotted in the Extended Data Figs. 2 and 3.

We use the ECS and TCR values for each model⁶ and diagnose A_{ze} and A_f from the CO₂ profiles (see Extended Data Fig. 4). The resultant theoretical estimates of ZEC are compared to the experimental values in Fig. 1. We find a close match between the normalized ZEC anticipated by the analytic model (Eqn. 4) and the normalized ZEC realized in the ESM simulations. The theoretical formula yields values that are on average within 0.11 of the experimental ZEC/T_{ze} , and, with a Pearson's coefficient of $R = 0.87$, there is a strong correlation between the analytic and EMIC results.

Models on average moderately cooled, with a typical reduction in the temperature anomaly of $\sim 30\%$ from the peak found at the end of emissions. The UVic and Bern-5 models are the exceptions, and exhibit warming of up to $\sim 30\%$ after emissions cease. By alternately fixing the thermal disequilibrium and carbon uptake to the ensemble-mean values and applying the ZEC formula (equation 2), we find that the physical and carbon dynamics contribute

roughly equally to the ensemble’s spread (Extended Data Fig. 5). Regarding the physics uncertainty, note that while models disagree on ECS by a factor of roughly four, ZEC depends on TCR/ECS, and the strong covariation of TCR with ECS (Extended Data Fig. 6) blunts the impact of physics uncertainty on ZEC. The cause of UVic’s warming is a weak post-emissions uptake of carbon, which results in an anomalously high A_f/A_{ze} . The carbon uptake in Bern-5 is unremarkable, but the thermal disequilibrium (TCR/ECS) is the smallest in the ensemble, yielding warming.

While there is intermodel spread, a given model’s response is strongly correlated across the three cumulative emissions scenarios. In the ZEC formalism introduced here, the only variable that changes from scenario to scenario is the carbon disequilibrium. Extended Data Fig. 7 shows that A_{ze} stabilizes at approximately the same value in a given model across the three scenarios, despite the variation in the cumulative emissions from 750 GtC to 2000 GtC. This behavior is also found in idealized carbon box models¹⁵, where the airborne fraction is a constant for the special case of exponential emissions, and the value is set by the emissions growth rate—1%/yr for the ZECMIP scenarios analyzed here. In terms of the governing variables for the zero-emissions commitment then, all three scenarios share identical values of thermal disequilibrium (fixed by the model’s TCR/ECS) and similar values of carbon disequilibrium (A_f/A_{ze}). This finding explains the general uniformity in a model’s response in Fig. 1 and in past studies⁵ of ZEC using 1%/yr forcings.

Comparison to the ZECMIP data builds confidence that Eqn. 2 faithfully represents the climate’s response to emissions cessation. Past work⁶ has used these model responses to 1%/yr forcings to infer the zero-emissions commitment for historical emissions. The view developed here stresses that ZEC depends on the airborne fraction and thus the rate of emissions, which varies between historical and 1%/yr runs. Given the ZEC formula, we can account for this difference and directly evaluate the historical ZEC.

Present-day committed warming

As in the 1%/yr case, evidence for negligible deep ocean warming for historical emissions comes from simulations^{12,20} in which the forcing is abruptly zeroed, and the temperature rapidly returns to near pre-industrial levels. This observation justifies the application of the ZEC formula to the historical case.

To compute the present-day ZEC, two additional quantities are needed: the thermal disequilibrium TCR/ECS and the final carbon airborne fraction. To estimate A_f for historical emissions, we note that A_f is expected from theory¹⁶ to depend linearly on C_{emit} , which is confirmed by the ZECMIP results (Extended Data Fig. 4). We evaluate the linear A_f fit for each ZECMIP model at $C_{emit} = 700$ GtC, and compute ZEC/T_{ze} via the analytic formula (Eqn. 4) with each model’s respective thermal disequilibrium. Averaging over the ZECMIP ensemble, we find $ZEC/T_{ze} = -11\%$ for historical emissions. For the 1%/yr simulations, the ensemble-mean cooling is $ZEC/T_{ze} = -33\%$ given 750 GtC of total emissions (Fig. 1), confirming our expectation that a 1%/yr run overestimates post-emissions cooling.

Another bias present in this calculation is that ZECMIP models are EMICS, which on average have higher TCR/ECS values than the CMIP6 ensemble⁸. Fig. 2 plots the predicted ZEC over a range of thermal disequilibria. For context, we plot the TCR/ECS values of the full CMIP6 ensemble²¹ in addition to ZECMIP⁶. Computing ZEC with the ensemble-mean thermal disequilibrium

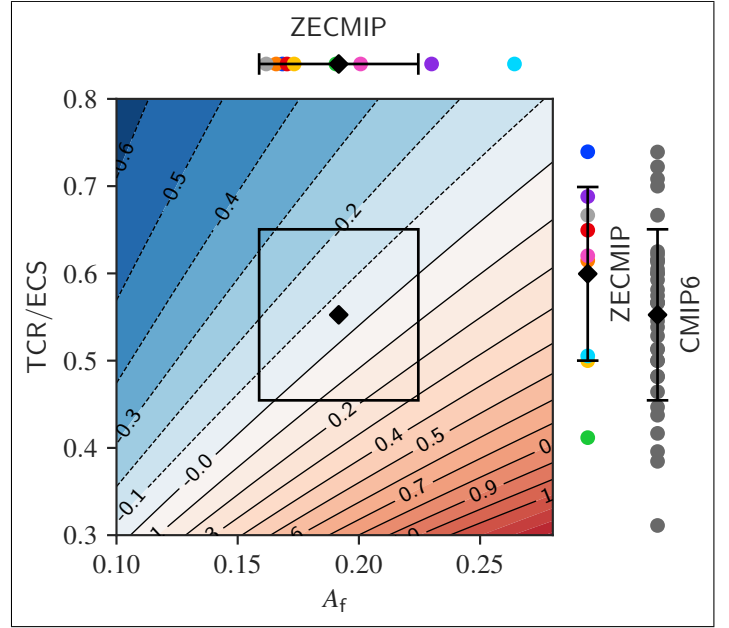


Fig. 2 | ZEC theory applied to historical emissions. The zero-emissions commitment at present (relative to the current temperature T_{ze}) found by evaluating the analytical theory (Eqn. 2) as a function of the final airborne fraction and thermal disequilibrium TCR/ECS. CMIP6 ensemble values of the thermal disequilibrium (grey) and ZECMIP results (multi-colored) are shown along with their respective means (black diamonds) and std. deviations (whiskers).

of the CMIP6 models shifts the central estimate to a slight cooling of less than 5% from the present temperature anomaly. At a standard deviation from the mean result, the temperature change is $\pm 30\%$. Future warming of comparable magnitude to historical warming is only possible if an outlier TCR/ECS is paired with an outlier A_f . (Note that the correlation between A_f and TCR/ECS is not significant in the ZECMIP ensemble as shown in Extended Data Fig. 8.) Because an outlier that is roughly two standard deviations from the ensemble averages is required, we conclude that substantial post-emissions warming due to historical emissions is unlikely.

Discussion

The idealized theory shows that committed warming arises from comparing the carbon disequilibrium at the time of emissions cessation to the model’s thermal disequilibrium. The current airborne fraction A_{ze} is near 0.4 given historical emissions. After land and ocean equilibration, the final airborne fraction is expected to be $A_f \approx 0.2$. The carbon disequilibrium at present is therefore $A_f/A_{ze} \approx 1/2$. Combined with the CMIP6 best estimate of the thermal disequilibrium $TCR/ECS \approx 1/2$, we find that $ZEC/T_{ze} \approx (A_f/A_{ze})/(TCR/ECS) - 1 \approx 0$. We therefore expect that if emissions cease, the temperature will be roughly constant.

This finding depends on the airborne fraction at the time of zero emissions, which in turn depends on the rate of emissions. If the same total emissions were emitted at a faster rate, for instance, then the airborne fraction would be higher at zero emissions. According to the ZEC formalism developed here, an A_{ze} that is higher than the historical value of 0.4 brings about post-emissions cooling. For instance, an airborne fraction of 0.8 yields a long-term

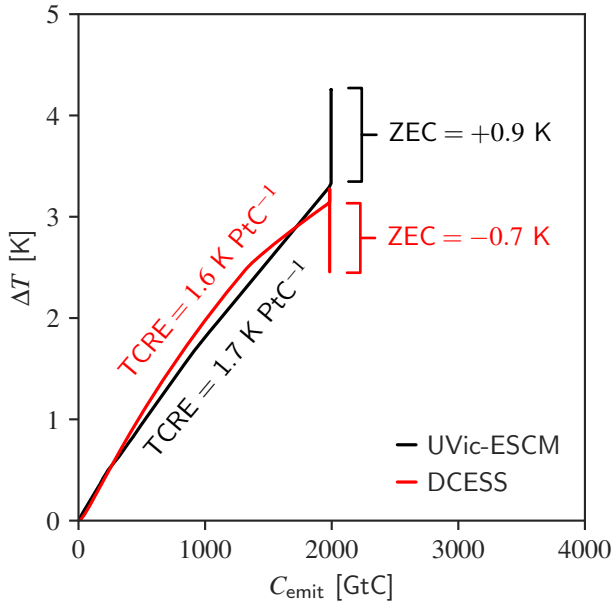


Fig. 3 | Contrasting TCRE and ZEC. The temperature response to cumulative emissions for a 1%/yr emissions scenario in UVic-ESCM (black) and DCESS (red). Models share a similar transient response during increasing emissions, but diverge after emissions end. ZEC captures this additional degree of freedom. DCESS and UVic-ESCM have the minimum and maximum ZEC, respectively, for the 2000 GtC case (Extended Data Fig. 2).

reduction of 50% from the temperature anomaly at zero emissions. On the other hand, if emissions are emitted more slowly than the historical rate, there is post-emissions warming: a temperature increase of over 50% occurs if A_{ze} is lowered from 0.4 to 0.25. This sensitivity to the airborne fraction at the time of cessation pushes back on the idea that there is a universal temperature response to emissions cessation, and hints that past results are dependent on the 1% per-year trajectories that have been frequently employed in the literature^{5,6,8,9,22}.

The existence of non-zero ZEC implies that the equilibrium response to cumulative emissions may differ from the transient response⁸. Fig. 3 highlights that models in ZECMIP can share similar transient responses to cumulative emissions (TCRE), but have divergent values of ZEC. In general, TCRE is poorly correlated with ZEC (Extended Data Fig. 1), and ZEC should be regarded as an independent degree of freedom. Budgeting carbon to achieve long-term temperature targets must therefore take into account both TCRE and ZEC^{2,3}.

The role of deep-ocean mixing in the uptake of both carbon and heat has in some cases^{5,23–25} been offered as justification for the absence of committed warming. A common timescale of uptake is cited as the reason why the decline in radiative forcing balances the decrease in heat loss to the deep ocean. This view, however, has drawn criticism²⁶ from process studies that reveal distinct ocean-uptake pathways for carbon and heat.

Here, we emphasize that even if deep ocean uptake of carbon and heat were identical, ZEC is not fully determined by this fact and may be far from zero. The key determinants of the post-emissions response are the thermal disequilibrium and carbon disequilibrium, and each are shaped at first order by processes unrelated to the deep ocean.

On the carbon side, land uptake is roughly equal to ocean up-

take¹⁴ over the historical period, but is notably absent from the prior timescales explanation. Regarding heat, the climate feedback parameter is equally as important as the ocean mixing rate in determining the thermal disequilibrium (Methods). Land uptake of carbon and the physical climate feedbacks are distinct in their origins, but essential to the post-emissions response and the central finding that $A_{ze}/A_f \approx \text{TCRE}/\text{ECS}$ for the historical case. Therefore, the lack of post-emissions temperature change for historical emissions is more aptly described as a coincidence, rather than as a consequence of ocean mixing.

Uncertainty in ZEC stems in roughly equal parts from uncertainty in carbon uptake and climate feedbacks (Extended Data Fig. 5). Improved confidence in our projections of land uptake, which drives carbon system uncertainty^{19,27,28}, and better constraints on cloud feedbacks—the leading source of climate feedback uncertainty^{29–31}—would directly improve the accuracy of ZEC estimates. Finally, the permanence of the long-term equilibrium depends on the rate at which sedimentary mixing and rock weathering restore the ocean’s alkalinity, facilitating the uptake of the remaining fossil fuels over tens of thousands of years¹⁷.

Several caveats to this work should be noted. We analyzed the climate response to only CO₂ emissions, and neglected the effects of methane, other greenhouse gases, and aerosols. However, prior work^{32,33} suggests that including these radiative forcings does not modify the first-order picture, as warming induced by aerosol reduction would be largely canceled by the cooling effect of methane’s decline if emissions end.

Finally, the ZEC formalism we developed is only applicable to emissions scenarios in which the deep ocean warming is small compared to the surface ocean warming when emissions end. This approximation holds for the historical case and the 1%/yr simulations analyzed here. For emissions that occur over multi-century timescales, however, the deep ocean warming may be comparable to that of the surface ocean. In this case, the formula provided here will underestimate the zero-emissions temperature T_{ze} , and can therefore be interpreted as providing an upper bound on ZEC, rather than a direct estimate. The sharpness of this bound for longer timescale emissions scenarios warrants further investigation.

Methods

Two-box model of climate

To examine the flow of heat, we use a simple two-box model^{11–13}. The lower box represents the deep ocean, and the upper box combines the ocean’s mixed layer and the atmosphere into a surface box. The internal energy of the surface box is dominated by the mixed layer, so we refer to the upper box as simply the surface ocean. Let T_s and T_d be the temperature deviation from the pre-industrial era of the ocean’s surface layer and deep interior, respectively. The energy budget of the upper box is approximated as

$$C_s \frac{dT_s}{dt} = F - \lambda T_s - \gamma(T_s - T_d), \quad (6)$$

where C_s is the mixed layer’s heat capacity (per area with units of J/K/m²), F is the radiative forcing (units of W/m²), and γ is the heat transfer coefficient between the two ocean layers (units of W/m²/K). The climate feedback parameter, which incorporates all feedback processes (Planck, water vapor, cloud, etc.), is parameterized as λT_s , where λ is the change in the top of atmosphere outgoing radiation per change in surface temperature. The

deep ocean's energy is governed by

$$C_d \frac{dT_d}{dt} = \gamma(T_s - T_d), \quad (7)$$

where C_d is the deep ocean's heat capacity. The box model's evolution consists of a fast and slow response to forcings¹², which we will briefly illustrate here. Consider applying a step function forcing to the surface ocean. Initially $T_d = 0$, and the forcing excites a surface layer response with timescale,

$$\tau_f = \frac{C_s}{\gamma + \lambda}. \quad (8)$$

Over timescales much larger than τ_f , we can neglect the tendency term in Equation 6, yielding a mixed layer in quasi-equilibrium at temperature

$$T_s \approx \frac{F + \gamma T_d}{\lambda + \gamma}. \quad (9)$$

In quasi-equilibrium, the deep layer budget is reduced to

$$\frac{dT_d}{dt} = -\frac{T_d}{\tau_s} + \frac{\gamma F}{(\lambda + \gamma)C_d}, \quad (10)$$

where we have defined the deep ocean's slow timescale of response,

$$\tau_s = \frac{(\lambda + \gamma)C_d}{\lambda \gamma}. \quad (11)$$

Climate models find timescales of $\tau_f \sim 5$ years and $\tau_s \sim 500$ years^{11,34,35}.

ZEC formula

Given the final radiative forcing F_f , energy balance constrains the final temperature,

$$T_f = \frac{F_f}{\lambda}. \quad (12)$$

Recalling that $\lambda \text{ ECS} = F_{2\times}$, where ECS is the equilibrium climate sensitivity for a doubling of a CO_2 , we have

$$T_f = \frac{F_f}{F_{2\times}} \text{ECS}. \quad (13)$$

Prior work^{8,36} has pointed out that we can simplify further by substituting in with the logarithmic radiative forcing expression,

$$F_f = F_0 \log \left(1 + A_f \frac{C_{\text{emit}}}{C_{\text{pre}}} \right), \quad (14)$$

where A_f is the fraction of anthropogenic cumulative emissions C_{emit} that remains in the atmosphere in the equilibrium state, F_0 is a constant, and $C_{\text{pre}} \approx 530 \text{ GtC}$ is the pre-industrial mass of atmospheric carbon¹⁴. We see that T_f is fully constrained by A_f and ECS^{22,24,37}.

For historical warming, we note that $T_s \gg T_d$ and the temperature response is well approximated¹² by

$$T_s \approx \frac{F}{\lambda + \gamma}. \quad (15)$$

We expect $T_s \gg T_d$ to also hold at the time of CO_2 doubling (year 70) following a 1%/yr increase in CO_2 concentration, as the duration of the forcing is small compared to the deep ocean response time. In this case, the surface temperature at the time of doubling

is known as the transient climate response (TCR), a standard metric tabulated for climate models. The contribution to TCR from the "recalcitrant warming" of the deep ocean has been probed by abruptly returning to pre-industrial forcing after year 70: T_d appears to be an order of magnitude less than TCR²⁰. We neglect T_d and approximate

$$\text{TCR} \approx \frac{F_{2\times}}{\lambda + \gamma}. \quad (16)$$

For a general emissions pathway, if the deep ocean anomaly is small compared to the surface anomaly at the time of emissions cessation, the temperature T_{ze} is approximately related to TCR via

$$\frac{T_{ze}}{\text{TCR}} \approx \frac{F_{ze}}{F_{2\times}} \approx \frac{\log(1 + A_{ze} C_{\text{emit}}/C_{\text{pre}})}{\log(2)}, \quad (17)$$

where A_{ze} is the cumulative airborne fraction when emissions are zeroed. Substituting our expressions for T_{ze} and T_f into the definition of ZEC, we arrive at our main result:

$$\text{ZEC} = \frac{1}{\log 2} \left[\log \left(1 + \frac{A_f C_{\text{emit}}}{C_{\text{pre}}} \right) \text{ECS} - \log \left(1 + \frac{A_{ze} C_{\text{emit}}}{C_{\text{pre}}} \right) \text{TCR} \right]. \quad (18)$$

Finally, we note that the thermal disequilibrium in the two-box model is given by $\text{TCR}/\text{ECS} = \lambda/(\lambda + \gamma)$.

ZECMIP computations

To account for natural variability, the zero-emissions temperature T_{ze} is taken to be the 20-year average centered on the time of zero emissions. The final temperature T_f is the average over the last 20 years in each simulation. The ZECMIP emissions are diagnosed by reconstructing the annual carbon budget,

$$\frac{\Delta \text{CO}_2}{\Delta t} = E - U, \quad (19)$$

where E is the emissions in GtC/yr , U is the combined land and ocean uptake in GtC/yr for each model, and CO_2 is the atmospheric mass of carbon-dioxide in GtC . The atmospheric tendency is equal to $\log(1.01) \text{ CO}_2/\text{yr}$ and the annual time series of CO_2 and U are reported for each model, enabling the determination of the annual emissions. The cumulative emissions up to time t are given by

$$C_{\text{emit}}(t) = \int_0^t E dt, \quad (20)$$

and the cumulative airborne fractions are defined as $A(t) = \text{CO}_2(t)/C_{\text{emit}}$ and shown in Extended Data Fig. 7. We analyze the subset of models in ZECMIP⁶ that simulated the millennial temperature response: Bern three-dimensional Earth System Model (Bern); Danish Centre for Earth System Science Earth System Model (DCESS); A.M. Obukhov Institute of Atmospheric Physics, Russian Academy of Sciences (IAPRAS); Loch-Vecode-ECbilt-Clio Model (LOVECLIM); Massachusetts Institute of Technology Earth System Model (MESM); Model for Interdisciplinary Research on Climate-lite/Japan Uncertainty Modelling Project Loosely Coupled Model (MIROC-lite); Planet Simulator – Grid-Enabled Integrated Earth system model (P. GENIE); and (8) University of Victoria Earth System Climate Model version 2.10 (UVic). Data from P. GENIE was excluded from the ZEC analysis due to a physical inconsistency identified in the temperature response (Extended Data Fig. 9).

Data availability

All of the data used in this study is made openly available by the ZECMIP collaboration at <http://terra.seos.uvic.ca/ZECMIP/Data/>.

Code availability

Code to reproduce the analysis and figures is archived at <https://zenodo.org/record/6410324>.

Acknowledgments

NT is supported by the National Science Foundation under grant 2127071 and a graduate research grant from the H2H8 foundation. The authors thank Aaron Match and Emma Ignazewski for helpful feedback on the manuscript.

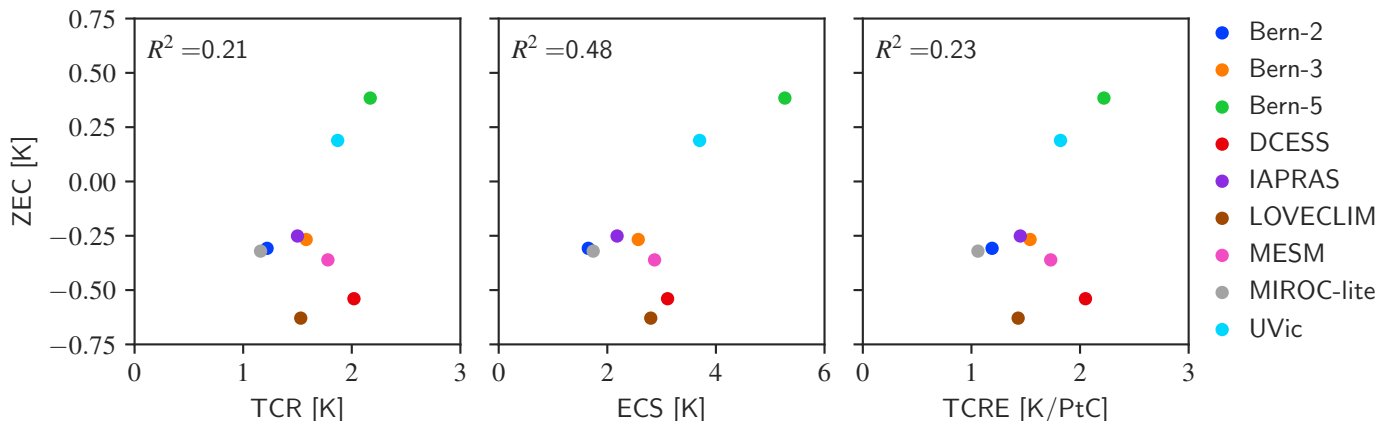
Contributions

N.T., N.J., and I.F. designed research; N.T. derived the two-box ZEC formalism, performed the analysis, and wrote the manuscript; and N.T., N.J. and I.F. contributed to the interpretation of the results, and revised the manuscript.

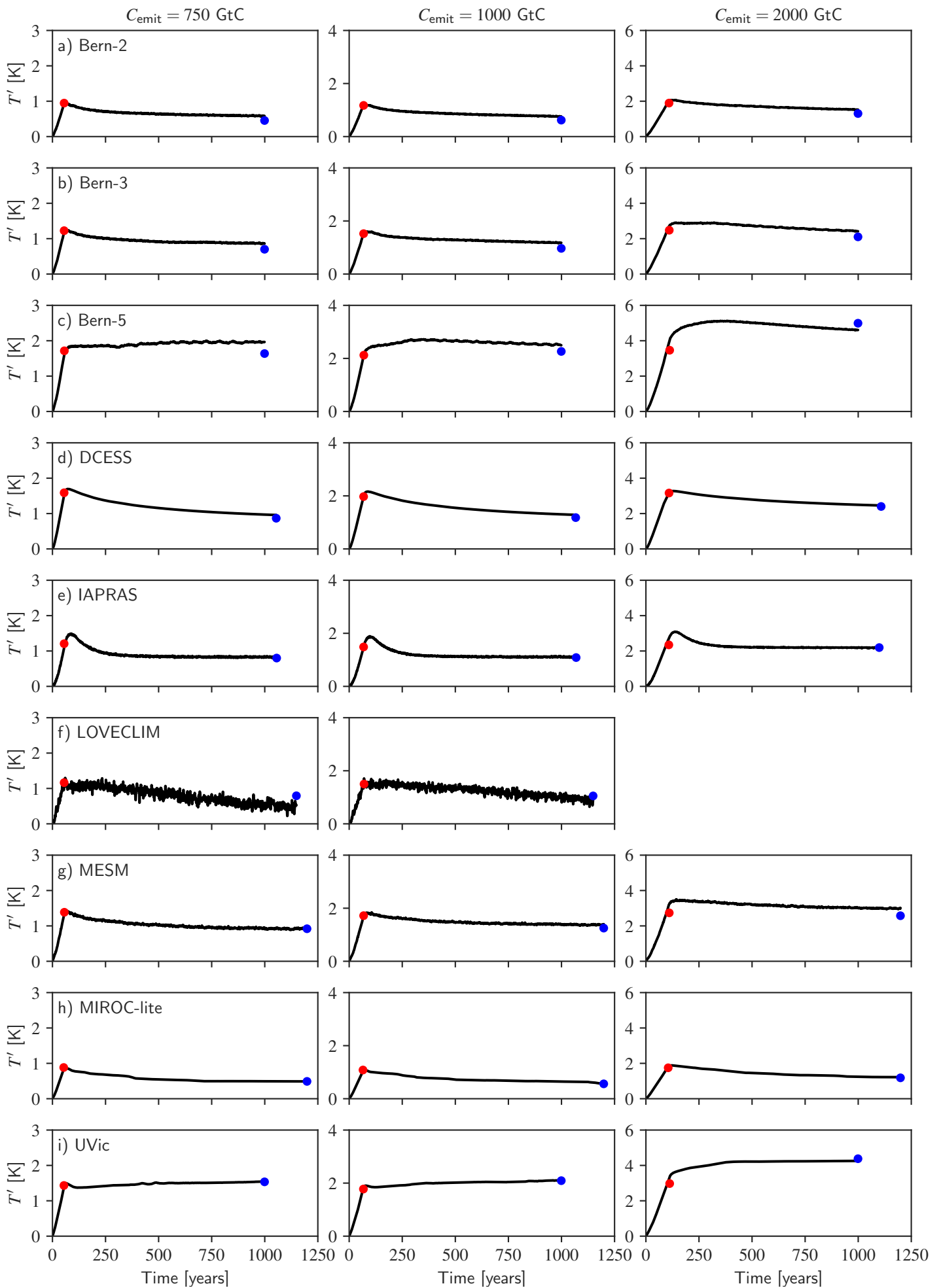
References

- [1] I. P. on Climate Change, *Climate Change 2013 – The Physical Science Basis: Working Group I Contribution to the Fifth Assessment Report of the Intergovernmental Panel on Climate Change*. Cambridge University Press, 2014.
- [2] J. Rogelj, P. M. Forster, E. Kriegler, C. J. Smith, and R. Séférian, “Estimating and tracking the remaining carbon budget for stringent climate targets,” *Nature*, vol. 571, no. 7765, pp. 335–342, 2019.
- [3] H. Damon Matthews, K. B. Tokarska, J. Rogelj, C. J. Smith, A. H. MacDougall, K. Haustein, N. Mengis, S. Sippel, P. M. Forster, and R. Knutti, “An integrated approach to quantifying uncertainties in the remaining carbon budget,” *Communications Earth & Environment*, vol. 2, no. 1, pp. 1–11, 2021.
- [4] H. D. Matthews and K. Caldeira, “Stabilizing climate requires near-zero emissions,” *Geophysical Research Letters*, vol. 35, no. 4, 2008.
- [5] S. Solomon, G.-K. Plattner, R. Knutti, and P. Friedlingstein, “Irreversible climate change due to carbon dioxide emissions,” *Proceedings of the national academy of sciences*, vol. 106, no. 6, pp. 1704–1709, 2009.
- [6] A. H. MacDougall, T. L. Frölicher, C. D. Jones, J. Rogelj, H. D. Matthews, K. Zickfeld, V. K. Arora, N. J. Barrett, V. Brovkin, F. A. Burger, M. Eby, A. V. Eliseev, T. Hajima, P. B. Holden, A. Jeltsch-Thömmes, C. Koven, N. Mengis, L. Menviel, M. Michou, I. I. Mokhov, A. Oka, J. Schwinger, R. Séférian, G. Shaffer, A. Sokolov, K. Tachiiri, J. Tjiputra, A. Wiltshire, and T. Ziehn, “Is there warming in the pipeline? a multi-model analysis of the zero emissions commitment from CO₂,” *Biogeosciences*, vol. 17, no. 11, pp. 2987–3016, 2020.
- [7] M. Collins, R. Knutti, J. Arblaster, J.-L. Dufresne, T. Fichefet, P. Friedlingstein, X. Gao, W. J. Gutowski, T. Johns, G. Krinner, *et al.*, “Long-term climate change: projections, commitments and irreversibility,” in *Climate Change 2013-The Physical Science Basis: Contribution of Working Group I to the Fifth Assessment Report of the Intergovernmental Panel on Climate Change*, pp. 1029–1136, Cambridge University Press, 2013.
- [8] T. L. Frolicher and D. J. Paynter, “Extending the relationship between global warming and cumulative carbon emissions to multi-millennial timescales,” *Environmental Research Letters*, vol. 10, p. 075002, jul 2015.
- [9] D. Ehlert and K. Zickfeld, “What determines the warming commitment after cessation of CO₂ emissions?,” *Environmental Research Letters*, vol. 12, p. 015002, jan 2017.
- [10] B. Hare and M. Meinshausen, “How much warming are we committed to and how much can be avoided?,” *Climatic Change*, vol. 75, no. 1, pp. 111–149, 2006.
- [11] J. M. Gregory, “Vertical heat transports in the ocean and their effect on time-dependent climate change,” *Climate Dynamics*, vol. 16, no. 7, pp. 501–515, 2000.
- [12] I. M. Held, M. Winton, K. Takahashi, T. Delworth, F. Zeng, and G. K. Vallis, “Probing the fast and slow components of global warming by returning abruptly to preindustrial forcing,” *Journal of Climate*, vol. 23, no. 9, pp. 2418–2427, 2010.
- [13] N. Jeevanjee, “The physics of climate change: simple models in climate science,” *arXiv preprint arXiv:1802.02695*, 2018.
- [14] P. Friedlingstein, M. O’Sullivan, M. W. Jones, R. M. Andrew, J. Hauck, A. Olsen, G. P. Peters, W. Peters, J. Pongratz, S. Sitch, C. Le Quééré, J. G. Canadell, P. Ciais, R. B. Jackson, S. Alin, L. E. O. C. Aragão, A. Arneeth, V. Arora, N. R. Bates, M. Becker, A. Benoit-Cattin, H. C. Bittig, L. Bopp, S. Bultan, N. Chandra, F. Chevallier, L. P. Chini, W. Evans, L. Florentie, P. M. Forster, T. Gasser, M. Gehlen, D. Gilfillan, T. Gkritzalis, L. Gregor, N. Gruber, I. Harris, K. Hartung, V. Haverd, R. A. Houghton, T. Ilyina, A. K. Jain, E. Joetzjer, K. Kadono, E. Kato, V. Kitidis, J. I. Korsbakken, P. Landschützer, N. Lefèvre, A. Lenton, S. Lienert, Z. Liu, D. Lombardozzi, G. Marland, N. Metz, D. R. Munro, J. E. M. S. Nabel, S.-I. Nakaoka, Y. Niwa, K. O’Brien, T. Ono, P. I. Palmer, D. Pierrot, B. Poulter, L. Resplandy, E. Robertson, C. Rödenbeck, J. Schwinger, R. Séférian, I. Skjelvan, A. J. P. Smith, A. J. Sutton, T. Tanhua, P. P. Tans, H. Tian, B. Tilbrook, G. van der Werf, N. Vuichard, A. P. Walker, R. Wanninkhof, A. J. Watson, D. Willis, A. J. Wiltshire, W. Yuan, X. Yue, and S. Zaehle, “Global carbon budget 2020,” *Earth System Science Data*, vol. 12, no. 4, pp. 3269–3340, 2020.
- [15] M. R. Raupach, “The exponential eigenmodes of the carbon-climate system, and their implications for ratios of responses to forcings,” *Earth System Dynamics*, vol. 4, no. 1, pp. 31–49, 2013.
- [16] P. Goodwin, R. G. Williams, M. J. Follows, and S. Dutkiewicz, “Ocean-atmosphere partitioning of anthropogenic carbon dioxide on centennial timescales,” *Global Biogeochemical Cycles*, vol. 21, no. 1, 2007.

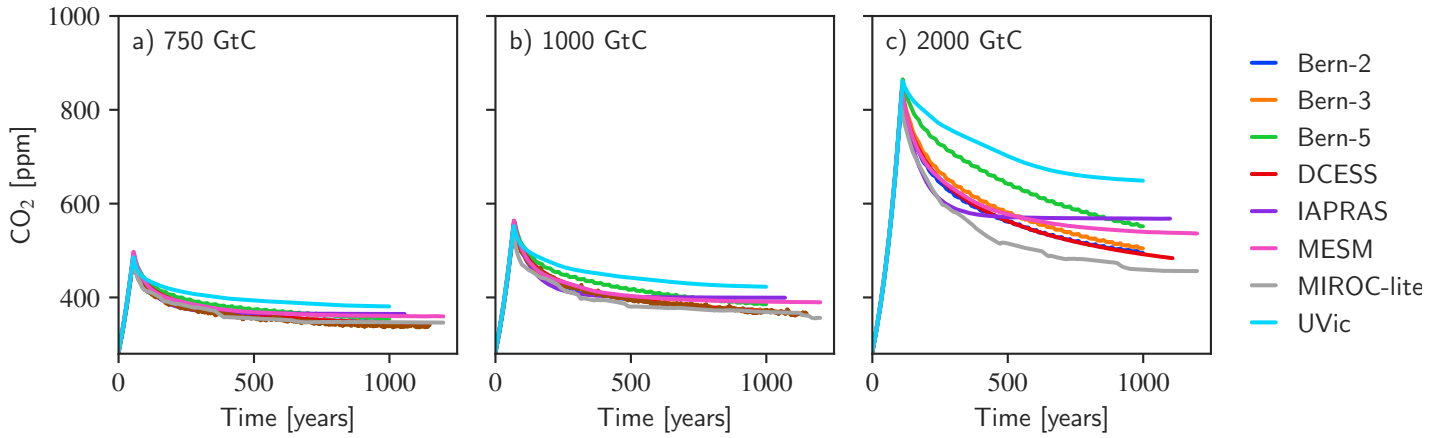
- [17] D. Archer, M. Eby, V. Brovkin, A. Ridgwell, L. Cao, U. Mikolajewicz, K. Caldeira, K. Matsumoto, G. Munhoven, A. Montenegro, *et al.*, “Atmospheric lifetime of fossil fuel carbon dioxide,” *Annual review of earth and planetary sciences*, vol. 37, pp. 117–134, 2009.
- [18] P. Friedlingstein, P. Cox, R. Betts, L. Bopp, W. von Bloh, V. Brovkin, P. Cadule, S. Doney, M. Eby, I. Fung, *et al.*, “Climate–carbon cycle feedback analysis: results from the c4mip model intercomparison,” *Journal of climate*, vol. 19, no. 14, pp. 3337–3353, 2006.
- [19] V. K. Arora, G. J. Boer, P. Friedlingstein, M. Eby, C. D. Jones, J. R. Christian, G. Bonan, L. Bopp, V. Brovkin, P. Cadule, T. Hajima, T. Ilyina, K. Lindsay, J. F. Tjiputra, and T. Wu, “Carbon-concentration and carbon-climate feedbacks in cmip5 earth system models,” *Journal of Climate*, vol. 26, no. 15, pp. 5289 – 5314, 2013.
- [20] M. Winton, A. Adcroft, J. P. Dunne, I. M. Held, E. Shevliakova, M. Zhao, H. Guo, W. Hurlin, J. Krasting, T. Knutson, D. Paynter, L. G. Silvers, and R. Zhang, “Climate sensitivity of gfdl’s cm4.0,” *Journal of Advances in Modeling Earth Systems*, vol. 12, no. 1, p. e2019MS001838, 2020.
- [21] G. A. Meehl, C. A. Senior, V. Eyring, G. Flato, J.-F. Lamarque, R. J. Stouffer, K. E. Taylor, and M. Schlund, “Context for interpreting equilibrium climate sensitivity and transient climate response from the cmip6 earth system models,” *Science Advances*, vol. 6, no. 26, p. eaba1981, 2020.
- [22] R. G. Williams, V. Roussenov, T. L. Frölicher, and P. Goodwin, “Drivers of continued surface warming after cessation of carbon emissions,” *Geophysical Research Letters*, vol. 44, no. 20, pp. 10,633–10,642, 2017.
- [23] H. D. Matthews and A. J. Weaver, “Committed climate warming,” *Nature Geoscience*, vol. 3, no. 3, pp. 142–143, 2010.
- [24] P. Goodwin, R. G. Williams, and A. Ridgwell, “Sensitivity of climate to cumulative carbon emissions due to compensation of ocean heat and carbon uptake,” *Nature Geoscience*, vol. 8, no. 1, pp. 29–34, 2015.
- [25] T. Mauritsen and R. Pincus, “Committed warming inferred from observations,” *Nature Climate Change*, vol. 7, no. 9, pp. 652–655, 2017.
- [26] T. L. Frolicher, J. L. Sarmiento, D. J. Paynter, J. P. Dunne, J. P. Krasting, and M. Winton, “Dominance of the southern ocean in anthropogenic carbon and heat uptake in cmip5 models,” *Journal of Climate*, vol. 28, no. 2, pp. 862 – 886, 2015.
- [27] D. Huntzinger, A. Michalak, C. Schwalm, P. Ciais, A. King, Y. Fang, K. Schaefer, Y. Wei, R. Cook, J. Fisher, *et al.*, “Uncertainty in the response of terrestrial carbon sink to environmental drivers undermines carbon-climate feedback predictions,” *Scientific reports*, vol. 7, no. 1, pp. 1–8, 2017.
- [28] N. S. Lovenduski and G. B. Bonan, “Reducing uncertainty in projections of terrestrial carbon uptake,” *Environmental Research Letters*, vol. 12, p. 044020, apr 2017.
- [29] P. M. Caldwell, M. D. Zelinka, K. E. Taylor, and K. Marvel, “Quantifying the sources of intermodel spread in equilibrium climate sensitivity,” *Journal of Climate*, vol. 29, no. 2, pp. 513–524, 2016.
- [30] P. Ceppi, F. Brient, M. D. Zelinka, and D. L. Hartmann, “Cloud feedback mechanisms and their representation in global climate models,” *Wiley Interdisciplinary Reviews: Climate Change*, vol. 8, no. 4, p. e465, 2017.
- [31] S. C. Sherwood, M. J. Webb, J. D. Annan, K. C. Armour, P. M. Forster, J. C. Hargreaves, G. Hegerl, S. A. Klein, K. D. Marvel, E. J. Rohling, M. Watanabe, T. Andrews, P. Braconnot, C. S. Bretherton, G. L. Foster, Z. Hausfather, A. S. von der Heydt, R. Knutti, T. Mauritsen, J. R. Norris, C. Proistosescu, M. Rugenstein, G. A. Schmidt, K. B. Tokarska, and M. D. Zelinka, “An assessment of earth’s climate sensitivity using multiple lines of evidence,” *Reviews of Geophysics*, vol. 58, no. 4, 2020.
- [32] C. J. Smith, P. M. Forster, M. Allen, J. Fuglestedt, R. J. Millar, J. Rogelj, and K. Zickfeld, “Current fossil fuel infrastructure does not yet commit us to 1.5 °c warming,” *Nature Communications*, vol. 10, no. 1, p. 101, 2019.
- [33] H. D. Matthews and K. Zickfeld, “Climate response to zeroed emissions of greenhouse gases and aerosols,” *Nature Climate Change*, vol. 2, no. 5, pp. 338–341, 2012.
- [34] D. J. L. Olivié, G. P. Peters, and D. Saint-Martin, “Atmosphere response time scales estimated from aogcm experiments,” *Journal of Climate*, vol. 25, no. 22, pp. 7956–7972, 2012.
- [35] O. Geoffroy, D. Saint-Martin, D. J. L. Olivié, A. Voldoire, G. Bellon, and S. Tytéca, “Transient climate response in a two-layer energy-balance model. part i: Analytical solution and parameter calibration using cmip5 aogcm experiments,” *Journal of Climate*, vol. 26, no. 6, pp. 1841–1857, 2013.
- [36] R. G. Williams, P. Goodwin, A. Ridgwell, and P. L. Woodworth, “How warming and steric sea level rise relate to cumulative carbon emissions,” *Geophysical Research Letters*, vol. 39, no. 19, 2012.
- [37] R. G. Williams, P. Goodwin, A. Ridgwell, and P. L. Woodworth, “How warming and steric sea level rise relate to cumulative carbon emissions,” *Geophysical Research Letters*, vol. 39, no. 19, 2012.



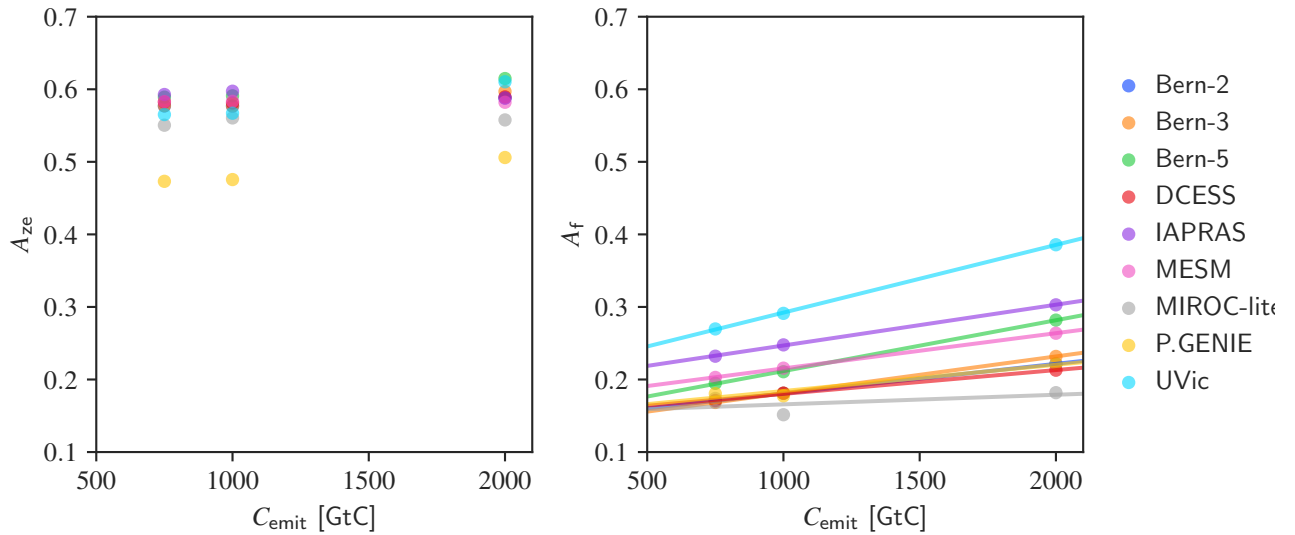
Extended Data Fig. 1 | ZEC correlates poorly with established metrics. Correlations between ZEC and the transient climate response (left), equilibrium climate sensitivity (center), and the transient climate response to cumulative emissions (right) are weak in the ZECMIP simulations. ZEC data corresponds to the 750 GtC cumulative emissions scenario.



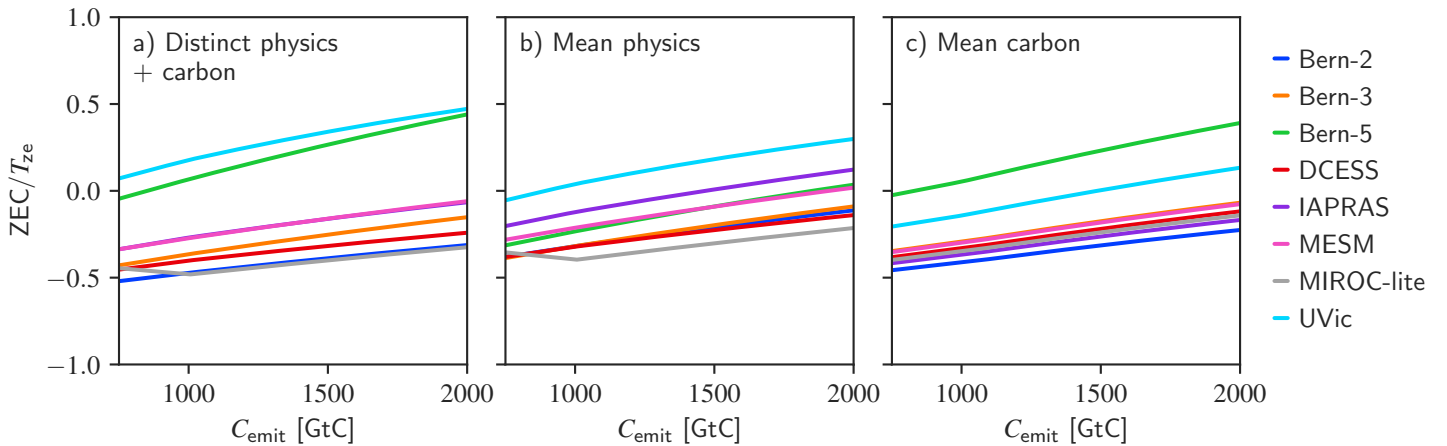
Extended Data Fig. 2 | Application of temperature scalings to ZECMIP. Per-model output (rows) is shown along with the analytic estimates of the zero-emissions temperature T_{ze} (red marker) and the final temperature T_f (blue marker) for cumulative emissions of 750 GtC (left), 1000 GtC (center), and 2000 GtC (right).



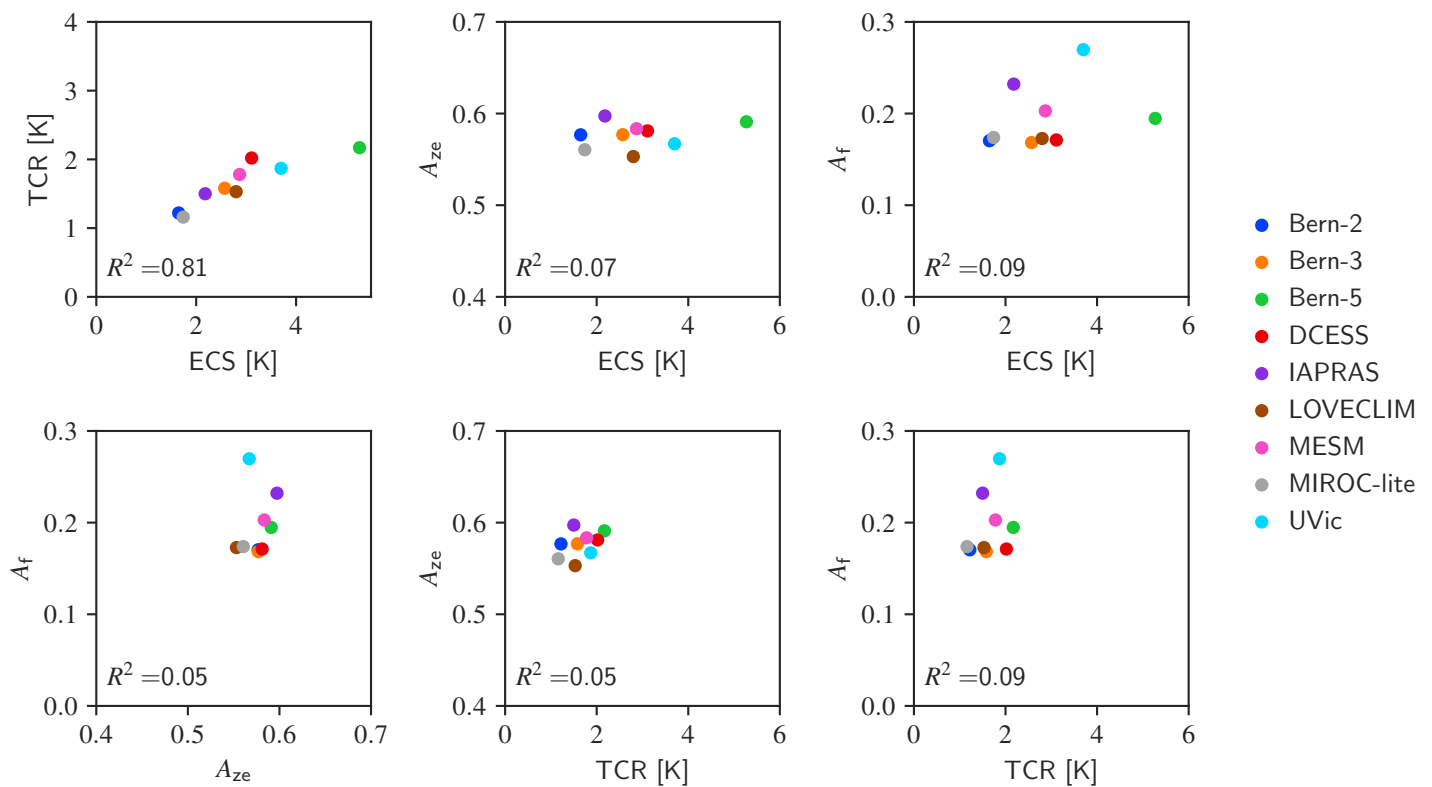
Extended Data Fig. 3 | Post-emissions CO_2 evolution. Atmospheric concentration of carbon dioxide in ZECMIP models for emissions pathways that yield a 1%/yr. growth in atmospheric carbon dioxide and cease at cumulative emissions of 750 GtC (left), 1000 GtC (center), and 2000 GtC (right).



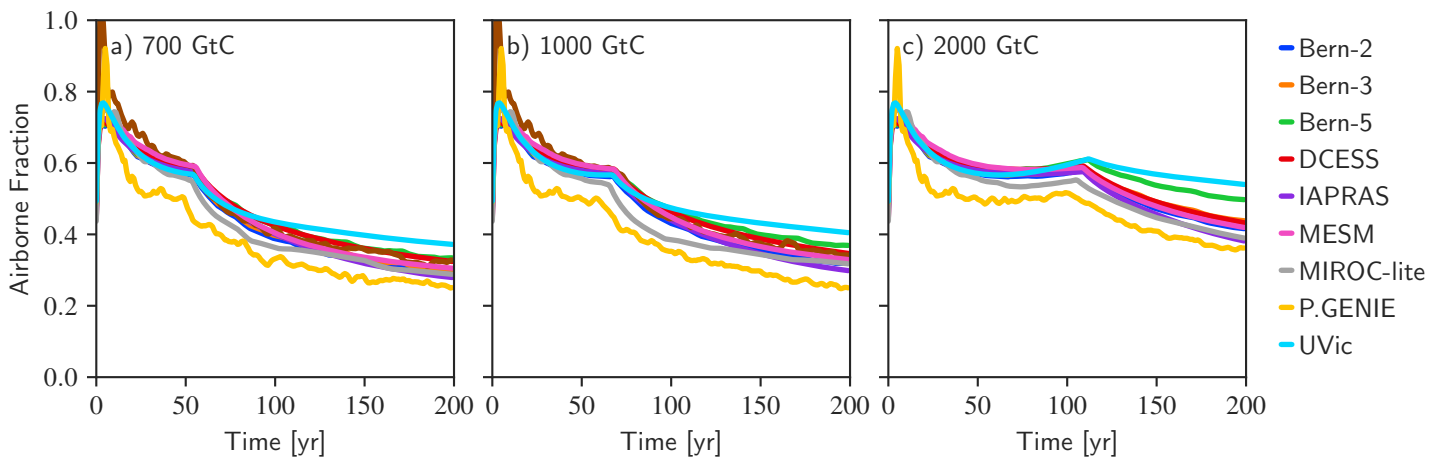
Extended Data Fig. 4 | Airborne fractions at zero-emissions and equilibrium. The airborne fraction at the time of emissions cessation (left) and in the final equilibrium (right) for different values of cumulative emissions in the ZECMIP simulation (scatter). Lines are least-squares fit to each model.



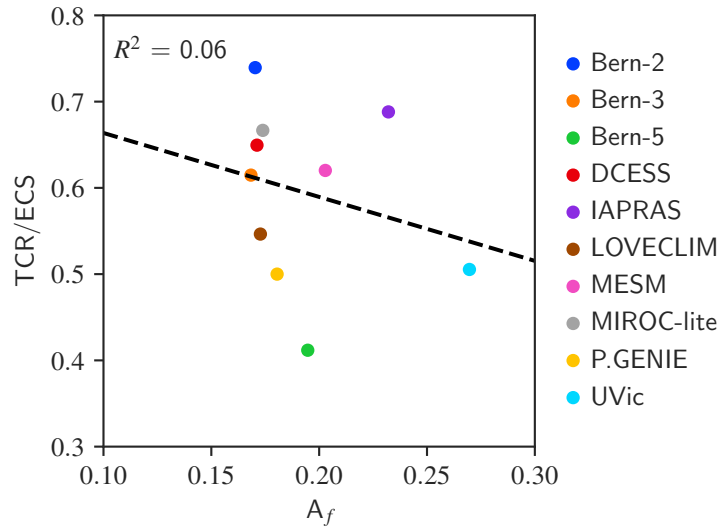
Extended Data Fig. 5 | ZEC variation due to carbon and physics uncertainty. ZEC responses computed analytically via equation 2 given a) each model's respective ECS, TCR, and airborne fractions; b) ensemble-mean ECS and TCR but per-model airborne fractions; and c) per-model ECS and TCR but ensemble-mean airborne fractions.



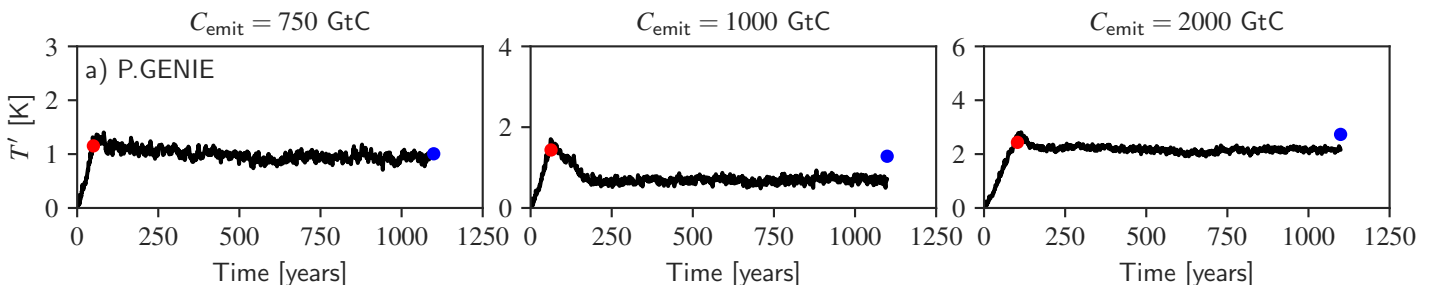
Extended Data Fig. 6 | Covariations between ZEC governing variables. Covariations between the ZEC governing parameters: equilibrium climate sensitivity (ECS), transient climate response (TCR), final airborne fraction (A_f), and the airborne fraction at zero-emissions (A_{ze}) in the ZECMIP ensemble. Airborne fractions correspond to the 750 GtC case. Only ECS and TCR exhibit substantial covariance.



Extended Data Fig. 7 | Equilibration of airborne fractions during emissions. Carbon airborne fractions for ZECMIP 1%/yr increase in CO_2 experiments followed by zero emissions after diagnosed cumulative emissions reach 750 GtC (left), 1000 GtC (center), and 2000 GtC (right). See methods for details on emissions reconstruction.



Extended Data Fig. 8 | Airborne fraction and thermal disequilibrium correlation. Correlation is weak ($R^2 = .06$) between the thermal disequilibrium and the final airborne fraction in the ZECMIP 750 GtC simulation.



Extended Data Fig. 9 | P. GENIE cools despite higher emissions. Same as Figure 2 but for the P. GENIE model. Note that the final temperature is lower for cumulative emissions of 1000 GtC (center) than 750 GtC (left). Decreasing equilibrium temperatures with increasing cumulative emissions is not physically plausible. Therefore, P. GENIE was excluded from the ZEC analysis presented here.